Fluid Antenna System For Anti-jamming Communication via Fast Port Switching

Junshan Luo, Zhengfei Qu, Hao Xu, Yonggang Zhu, Kai-Kit Wong, *Fellow, IEEE*, Hyundong Shin, *Fellow, IEEE*

***Abstract*—The fluid antenna system (FAS) holds big promise in wireless communications due to the ability of reconfiguring the antenna position to enhance the spatial diversity. In this paper, we propose an anti-jamming communication scheme that exploits the FAS to combat a malicious jammer, which intentionally sends jamming signals to interfere with the legitimate receiver. In contrast to the conventional anti-jamming communication schemes that rely on antenna arrays to mitigate the unintentional signals, the proposed scheme uses the FAS at the receiver side which has multiple open ports sharing a single radio-frequency chain. By rapidly switching the active port, the FAS receives multiple different faded signals which can be carefully combined to improve the desired signal strength and suppress the jamming signals. Considering the practical imperfections of the jamming channel, we formulate a worst-case achievable rate maximization problem by jointly designing the transmit beamforming and the receive combining coefficients, subject to the general power constraints. We derive the semi-closed-form solutions to the formulated non-convex problem, which remarkably reduces the computational complexity. Numerical results demonstrate the proposed scheme is robust to channel imperfection, and the achievable rate outperforms that of the conventional fixed-position antenna schemes which have multiple antennas and multiple radio frequency chains.**

***Index Terms*—Anti-jamming communication, fluid antenna system, port switching, receive combining, robust beamforming.**

I. Introduction

Wireless communication systems are inherently vulnerable to jamming attacks due to the open nature of wireless propagation. Conventional anti-jamming strategies such as frequency hopping (FH), direct-sequence spread spectrum (DSSS) [1], jamming cancellation [2] have been widely adopted to mitigate the intentional interference . In the spatial domain, beamforming with multiple-input multiple-output (MIMO) can be further incorporated to nullify jamming signals arriving from specific directions [3]. However, these methods often require multiple radio-frequency (RF) chains and dedicated modulators, leading to increased hardware cost, power consumption, and in the case of DSSS/FH, bandwidth expansion, making them less suitable for compact, energy-constrained devices.

Recently, the fluid antenna system (FAS) has emerged as a promising technology to enhance spatial diversity with limited RF chains [4]. By dynamically adjusting the active antenna port, the FAS can exploit channel variations to improve signal quality and mitigate interference. Although the concept of FAS was first mentioned in the antenna community [5], [6], only in recent years, the potential of the FAS to improve the performance of the wireless communications has been partially unveiled. Prior works on FAS have mainly focused on performance analysis [7], diversity gain [8], capacity optimization [9], physical layer security [10], [11], and integration with other advanced techniques [12], [13]. However, the potential of FAS for anti-jamming communication remains largely unexplored, particularly under practical impairments such as channel estimation errors. This constitutes a critical research gap, as the intrinsic ability of FAS to rapidly reconfigure its active ports and exploit deep fades in the jamming channel offers a fundamentally new pathway for interference suppression.

In this paper, motivated by the fact that the FAS provides increased spatial degree-of-freedom and can adjust the active port where the jamming signals suffer from deep fade, we propose an anti-jamming communication scheme based on the FAS, which consists of one RF chain, one radiating element, and multiple open ports. Specifically, we deploy the FAS at the receiver side, and the active port of the FAS is switched at the speed of sub-symbol level [14], such that differently faded signals can be received and deliberately combined to enhance the useful signals while suppressing the unintentional signals. While recent work on movable antennas (MA) [15]–[18] has explored antenna position optimization, this work proposes fast port switching to counter symbol-level agile jamming. Specifically, we aim to maximize the achievable rate by joint transmit beamforming and received sub-symbol combining, subject to the general power constraints [19] and jamming channel imperfection. Although the formulated problem is non-convex, we derive the optimal semi-closed-form solutions, which significantly reduces the computational complexity.

Compared with the conventional DSSS and FH, the proposed FAS requires a single RF chain while dedicated modulators are demanded for DSSS/FH. In addition, the proposed

The work of H. Xu was supported by National Natural Science Foundation of China under Grants 62501152 and U25A20398, and also by the Fundamental Research Funds for the Central Universities under grant 2242025R10001. (*Corresponding authors: Zhengfei Qu and Hao Xu.*)

Junshan Luo and Yonggang Zhu are with the Sixty-Third Research Institute, National University of Defense Technology, Nanjing 210007, China (e-mail: luojunshan10@nudt.edu.cn)

Zhengfei Qu is with the College of Electronic Science and Technology, National University of Defense Technology, Changsha 410005, China (e-mail: quzhengfei2023@163.com)

Hao Xu is with the National Mobile Communications Research Laboratory, Southeast University, Nanjing 210096, China (e-mail: hao.xu@seu.edu.cn)

Kai-Kit Wong is with the Department of Electronic and Electrical Engineering, University College London, WC1E 7JE London, U.K., and also with the Department of Electronic Engineering, Kyung Hee University, Yongin-si, Gyeonggi-do 17104, Republic of Korea. (e-mail: kai-kit.wong@ucl.ac.uk).

Hyundong Shin is with the Department of Electronics and Information Convergence Engineering, Kyung Hee University, Yongin-si, Gyeonggi-do 17104, Republic of Korea (e-mail: hshin@khu.ac.kr).

TABLE I
MAIN MATRIX NOTATIONS

Symbol	Definition	Dimension
$\boldsymbol{H}$	Equivalent legitimate channel matrix	$\mathbb{C}^{L\times N}$
$\boldsymbol{G}$	Equivalent jamming channel matrix	$\mathbb{C}^{L\times M}$
$\boldsymbol{\Lambda}$	Diagonal eigenvalue matrix of $\boldsymbol{J}$	$\mathbb{C}^{L\times L}$
$\boldsymbol{\Omega}_k$	Power constraint matrix for kth cluster	$\mathbb{C}^{N\times N}$
$\boldsymbol{J}$	Spatial correlation matrix	$\mathbb{C}^{L\times L}$

FAS does not incur bandwidth penalty, which is critical for crowded bands. Furthermore, the FAS can be layered with DSSS/FH for cross-domain robustness. For ease reference, we list the main variables used in this paper in Table I.

II. System Model and Problem Formulation

A. Signal and Channel Model

We consider the communication scenario where the transmitter attempts to send the desired signal to the receiver, while the malicious jammer tries to degrade the legitimate channel. The transmitter and the jammer are equipped with N and M fixed antennas, respectively. The receiver has a fluid antenna whose location can be switched rapidly to one of L predetermined open ports uniformly distributed over a length of $W\lambda$, where $W > 0$ represents the normalized length and λ denotes the wavelength.

Assume the signals of the transmitter and the jammer are $\boldsymbol{x} = \boldsymbol{w}_{\mathrm{U}} s_{\mathrm{U}}$ and $\boldsymbol{z} = \boldsymbol{w}_{\mathrm{J}} s_{\mathrm{J}}$, respectively, where $s_{\mathrm{U}} \sim \mathcal{CN}(0, p_{\mathrm{U}})$ is the useful signal, and $s_{\mathrm{J}} \sim \mathcal{CN}(0, p_{\mathrm{J}})$ is the jamming signal. p_{U} and p_{J} are the transmit powers. $\boldsymbol{w}_{\mathrm{U}} \in \mathbb{C}^N$ and $\boldsymbol{w}_{\mathrm{J}} \in \mathbb{C}^M$ denote the transmit and jamming beamforming vectors, respectively. To enhance the spatial degree-of-freedom for jamming mitigation, we equally divide one symbol period into L time slots.

During the l-th sub-symbol slot, $l = 1, 2, \cdots, L$, the l-th port is activated for signal receiving, and the received signal is expressed by

$$y_l = \boldsymbol{h}_l^{\dagger} \boldsymbol{x}^{(0)} e^{j\phi} + \beta \boldsymbol{h}_l^{\dagger} \boldsymbol{x}^{(-1)} e^{j\phi} + \boldsymbol{g}_l^{\dagger} \boldsymbol{z} + n_l, \tag{1}$$

where $\boldsymbol{x}^{(0)}$ and $\boldsymbol{x}^{(-1)}$ represent the current and previous symbols due to timing offset introduced by high-speed port switching; $\beta \in [0, 1]$ represents the inter-symbol interference (ISI) coefficient, where $\beta = 0$ denotes no ISI and $\beta = 1$ denotes complete overlapping; $\phi \in [0, 2\pi]$ denotes the phase misalignment; $\boldsymbol{h}_l \in \mathbb{C}^N$ denotes the channel between the transmitter and the receiver in the l-th time slot; $\boldsymbol{g}_l \in \mathbb{C}^M$ is defined similarly for the jamming channel; $n_l \sim \mathcal{CN}(0, \sigma^2)$ is the complex additive white Gaussian noise and σ^2 is the variance. The operator $(\cdot)^{\dagger}$ denotes conjugate transpose.

After L time slots, the receiver combines the received signals with a weighting coefficients vector $\boldsymbol{a}^{\dagger} = [a_1, a_2, \ldots, a_L]$ and obtains

$$y = \sum_{l=1}^{L} a_l y_l. \tag{2}$$

Substituting (1) into (2) yields

$$y = \boldsymbol{a}^{\dagger} \boldsymbol{H} \boldsymbol{x}^{(0)} e^{j\phi} + \beta \boldsymbol{a}^{\dagger} \boldsymbol{H} \boldsymbol{x}^{(-1)} e^{j\phi} + \boldsymbol{a}^{\dagger} \boldsymbol{G} \boldsymbol{z} + \boldsymbol{a}^{\dagger} \boldsymbol{n}, \tag{3}$$

where $\boldsymbol{H} = [\boldsymbol{h}_1, \boldsymbol{h}_2, \ldots, \boldsymbol{h}_L]^{\dagger} \in \mathbb{C}^{L\times N}$ represents the equivalent legitimate channel; $\boldsymbol{G} = [\boldsymbol{g}_1, \boldsymbol{g}_2, \ldots, \boldsymbol{g}_L]^{\dagger} \in \mathbb{C}^{L\times M}$ denotes the equivalent jamming channel; $\boldsymbol{n} = [n_1, n_2, \ldots, n_L]^{\mathrm{T}} \in \mathbb{C}^L$ is the noise vector following $\mathcal{CN}(\boldsymbol{0}, \sigma^2 \boldsymbol{I})$ with $\boldsymbol{I}$ being the identity matrix. For the FA, since the adjacent ports are close to each other, the channel gains at different ports are highly correlated. We use the widely acknowledged Jakes' assumption to model the cross correlation of the channels [20]. Specifically, for the legitimate channel, each column of $\boldsymbol{H}$ follows $\mathcal{CN}(\boldsymbol{0}, \boldsymbol{J})$. The (l, ℓ)-th element, $\ell = 1, 2, \cdots, L$, of the covariance matrix $\boldsymbol{J} \in \mathbb{C}^{L\times L}$ is expressed as

$$[\boldsymbol{J}]_{l,\ell} = J_0\Big(2\pi \frac{|l-\ell|}{L-1} W\Big), \tag{4}$$

where $J_0(\cdot)$ is the zero-order Bessel function of the first kind. As such, we have $\boldsymbol{H} = \boldsymbol{Q}\boldsymbol{\Lambda}^{\frac{1}{2}}\boldsymbol{V}$, where $\boldsymbol{Q} \in \mathbb{C}^{L\times L}$ is the eigenvector matrix of $\boldsymbol{J}$; $\boldsymbol{\Lambda} \in \mathbb{C}^{L\times L}$ is the diagonal eigenvalue matrix of $\boldsymbol{J}$; Each element of $\boldsymbol{V} \in \mathbb{C}^{L\times L}$ is independent and identically distributed and follows from $\mathcal{CN}(0, 1)$. The equivalent jamming channel $\boldsymbol{G}$ is defined in a similar fashion, which is omitted here for brevity.

From (3), the achievable rate at the user is simplified as[1]

$$R = \log_2\left(1 + \frac{p_{\mathrm{U}} |\boldsymbol{a}^{\dagger} \boldsymbol{H} \boldsymbol{w}_{\mathrm{U}}|^2}{p_{\mathrm{J}} |\boldsymbol{a}^{\dagger} \boldsymbol{G} \boldsymbol{w}_{\mathrm{J}}|^2 + p_{\mathrm{U}} \beta^2 c + \|\boldsymbol{a}\|^2 \sigma^2}\right), \tag{5}$$

where $c \triangleq \mathbb{E}\{|\boldsymbol{a}^{\dagger} \boldsymbol{H} \boldsymbol{w}_{\mathrm{U}}^{(-1)}|^2\}$ is a constant associated with $\boldsymbol{w}_{\mathrm{U}}^{(-1)}$, the transmit beamforming at the last slot. We assume that the legitimate channel $\boldsymbol{H}$ is perfectly known due to the cooperation between the transmitter and the receiver. However, obtaining the accurate jamming channel $\boldsymbol{G}$ is difficult. Note that since the jamming channel is highly related to the relative position between the jammer and the user, thus $\boldsymbol{G}$ can be roughly estimated by detecting the jamming power emitted from the jammer. We use the bounded CSI error model to represent the effect, i.e.,

$$\hat{\boldsymbol{G}} = \boldsymbol{G} + \boldsymbol{E}, \tag{6}$$

where $\|\boldsymbol{E}\| \leq \epsilon$ and $\epsilon > 0$ is an upper bound of the channel estimation error; $\|\cdot\|$ is the Frobenius norm. In practical anti-jamming systems where active channel estimation is infeasible, we can exploit the spatial correlation structure, e.g., the Jakes' model, to reconstruct the jamming channel from the received power measurements. This guarantees that the estimation error is bounded by ϵ, which derives from measurable noise statistics.

B. The Optimal Jamming Strategy

We assume that a powerful jammer has perfect global CSI and designs its beamforming strategy $\boldsymbol{w}_{\mathrm{J}}$ based on its perfect

[1]Note that the phase term $e^{j\phi}$ vanishes due to the modulus operation. However, the phase misalignment indeed affects the demodulation of the symbols. It requires accurate phase compensation methods for perfect symbol recovery. To enhance the robustness against phase misalignment, the adaptive switching granularity can be used, i.e., dynamically adjusting L based on channel coherence time. For example, smaller L is used in high-Doppler scenarios. Moreover, pre-calibration of phase shifts can also be used to compensate the hardware imperfections [21].

CSI and knowledge of the legitimate system's transmission strategy. Thus, for fixed $\boldsymbol{a}$ and $\boldsymbol{w}_{\mathrm{U}}$, the jammer can choose $\boldsymbol{w}_{\mathrm{J}}$ to minimize the achievable rate at the user based on the actual channels. Specifically, the jammer needs to solve the following problem

$$\sup_{\boldsymbol{w}_{\mathrm{J}}\in\mathcal{W}} |\boldsymbol{a}^{\dagger}\boldsymbol{G}\boldsymbol{w}_{\mathrm{J}}|^2, \tag{7}$$

where $\mathcal{W} \triangleq \{\boldsymbol{w}_{\mathrm{J}} \in \mathbb{C}^M | \|\boldsymbol{w}_{\mathrm{J}}\|^2 \leq 1\}$ is the feasible set of $\boldsymbol{w}_{\mathrm{J}}$. From the Cauchy-Schwarz inequality, the optimal solution to (7) is $\boldsymbol{w}_{\mathrm{J}}^* = \boldsymbol{G}^{\dagger}\boldsymbol{a}/\|\boldsymbol{a}^{\dagger}\boldsymbol{G}\|$. This jamming strategy provides a rigorous lower-bound performance metric for our proposed scheme under the most adversarial scenario.

C. Problem Formulation

We aim to maximize the minimum achievable rate at the user against malicious jamming, by jointly optimizing the transmitter's beamforming vector $\boldsymbol{w}_{\mathrm{U}}$ and the receiving weighting factors $\boldsymbol{a}$, subject to the general power constraints and the jamming CSI uncertainty. Specifically, the problem is formulated as

$$\max_{\boldsymbol{w}_{\mathrm{U}},\boldsymbol{a}} \quad \min_{\|\boldsymbol{E}\|\leq\epsilon} R \tag{8a}$$

$$\text{s.t.} \quad \boldsymbol{w}_{\mathrm{U}}^{\dagger}\boldsymbol{\Omega}_k\boldsymbol{w}_{\mathrm{U}} \leq p_k, \qquad \forall k = 1, 2, \ldots, K, \tag{8b}$$

$$\|\boldsymbol{a}\|^2 = 1, \tag{8c}$$

where constraints (8b) represent that the transmit antennas are divided into K clusters and the maximum transmit power of the k-th antenna cluster is p_k.[2] $\boldsymbol{\Omega}_k \in \mathbb{C}^{N\times N}$ models power amplifier constraints for antenna cluster k. Crucially, the model supports heterogeneity through asymmetric power constraints, flexible $\boldsymbol{\Omega}_k$ matrices enabling overlapping/non-uniform clusters, and compatibility with classic total-power constraints, e.g., for $K = 1$ and $\boldsymbol{\Omega}_k = \boldsymbol{I}$, constraint (8b) reduces to the conventional total power constraint. Constraint (8c) enforces power normalization on the combined signal, ensuring the achievable rate is well-defined and maintaining physical realism while preserving optimality. In the following, we use the alternating optimization framework to handle the non-convex problem (8).

III. Joint Transmit Beamforming and Receiving Weighting Factor Design

A. Transmit Beamforming Design

When $\boldsymbol{a}$ is fixed, the problem (8) is reduced to the following subproblem of optimizing $\boldsymbol{w}_{\mathrm{U}}$

$$\max_{\boldsymbol{w}_{\mathrm{U}}} \quad \mathrm{tr}\{\tilde{\boldsymbol{H}}\boldsymbol{W}_{\mathrm{U}}\} \tag{9a}$$

$$\text{s.t.} \quad \mathrm{tr}\{\boldsymbol{\Omega}_k\boldsymbol{W}_{\mathrm{U}}\} \leq p_k, \qquad \forall k = 1, 2, \ldots, K, \tag{9b}$$

$$\boldsymbol{W}_{\mathrm{U}} \succeq \boldsymbol{0}, \tag{9c}$$

$$\mathrm{rank}\{\boldsymbol{W}_{\mathrm{U}}\} = 1, \tag{9d}$$

[2]The cluster-based transmit structure models practical systems where antennas are grouped per physical constraints such as distributed antenna system where unmanned aerial vehicle (UAV) swarms with independent power amplifier per cluster, multi-panel base stations where antennas grouped per radio frequency chain, collaborative Internet of Things (IoT) devices with local energy budget, etc.

where $\tilde{\boldsymbol{H}} \triangleq \boldsymbol{H}^{\dagger}\boldsymbol{a}\boldsymbol{a}^{\dagger}\boldsymbol{H} \in \mathbb{C}^{N\times N}$ and $\boldsymbol{W}_{\mathrm{U}} \triangleq \boldsymbol{w}_{\mathrm{U}}\boldsymbol{w}_{\mathrm{U}}^{\dagger} \in \mathbb{C}^{N\times N}$. Constraints (9c) and (9d) derive from the definition of $\boldsymbol{W}_{\mathrm{U}}$. Constraint (9b) is obtained from (8b), which is intractable for deriving a closed-form solution of (9). However, note that the multiple power constraints can be equivalently transformed into a single unified power constraint, i.e.,

$$\mathrm{tr}\{\boldsymbol{\Upsilon}\boldsymbol{W}_{\mathrm{U}}\} \leq P, \tag{10}$$

where $P = \sum_{k=1}^{K} p_k$ is the total power budget; $\boldsymbol{\Upsilon} \triangleq \sum_{k=1}^{K} \theta_k\boldsymbol{\Omega}_k$; $\theta_k = \eta_k P/\sum_{\kappa=1}^{K}\eta_\kappa p_\kappa$ is the weighting factor and $\eta_k \geq 0$ is the optimal dual variable. The dual problem of (9) can be formulated to find the solution of η_k, i.e.,

$$\min_{\boldsymbol{Q},\{\eta_k\}} \quad \sum_{k=1}^{K}\eta_k p_k \tag{11a}$$

$$\text{s.t.} \quad \sum_{k=1}^{K}\eta_k\boldsymbol{\Omega}_k - \tilde{\boldsymbol{H}} - \boldsymbol{Q} \succeq \boldsymbol{0}, \tag{11b}$$

where $\boldsymbol{Q} \succeq \boldsymbol{0}$ is the dual matrix associated with $\boldsymbol{W}_{\mathrm{U}}$. Note that problem (11) is convex and can thus be efficiently solved by CVX. Using (10) and defining $\boldsymbol{W}_{\mathrm{U}} \triangleq \boldsymbol{\Upsilon}^{-\frac{1}{2}}\tilde{\boldsymbol{W}}_{\mathrm{U}}\boldsymbol{\Upsilon}^{-\frac{1}{2}}$, problem (9) can be equivalently rewritten as

$$\max_{\tilde{\boldsymbol{W}}_{\mathrm{U}}} \quad \mathrm{tr}\{\tilde{\boldsymbol{H}}\boldsymbol{\Upsilon}^{-\frac{1}{2}}\tilde{\boldsymbol{W}}_{\mathrm{U}}\boldsymbol{\Upsilon}^{-\frac{1}{2}}\} \tag{12a}$$

$$\text{s.t.} \quad \mathrm{tr}\{\tilde{\boldsymbol{W}}_{\mathrm{U}}\} \leq P, \tag{12b}$$

$$\tilde{\boldsymbol{W}}_{\mathrm{U}} \succeq \boldsymbol{0}, \tag{12c}$$

$$\mathrm{rank}\{\tilde{\boldsymbol{W}}_{\mathrm{U}}\} = 1, \tag{12d}$$

which takes a similar form of a classical MIMO capacity maximization problem. The optimal solution is $\tilde{\boldsymbol{W}}_{\mathrm{U}} = P\boldsymbol{u}_{\max}\boldsymbol{u}_{\max}^{\dagger}$, where $\boldsymbol{u}_{\max}$ denotes the eigenvector corresponding to the largest eigenvalue of $\boldsymbol{\Upsilon}^{-\frac{1}{2}}\tilde{\boldsymbol{H}}\boldsymbol{\Upsilon}^{-\frac{1}{2}}$. Recalling the definitions of $\boldsymbol{W}_{\mathrm{U}}$, we have the optimal semi-closed-form solution to problem (9), i.e.,

$$\boldsymbol{w}_{\mathrm{U}} = \sqrt{P}\boldsymbol{\Upsilon}^{-\frac{1}{2}}\boldsymbol{u}_{\max}. \tag{13}$$

B. Receiving Weighting Factors Design

When $\boldsymbol{w}_{\mathrm{U}}$ is fixed, the problem (8) can be reformulated as the following max-min subproblem of optimizing $\boldsymbol{a}$

$$\max_{\boldsymbol{a}} \quad \min_{\|\boldsymbol{E}\|\leq\epsilon} \frac{p_{\mathrm{U}}|\boldsymbol{a}^{\dagger}\boldsymbol{H}\boldsymbol{w}_{\mathrm{U}}|^2}{p_{\mathrm{J}}\|\boldsymbol{a}^{\dagger}\hat{\boldsymbol{G}}\|^2 + p_{\mathrm{U}}\beta^2 c + \sigma^2} \tag{14}$$

$$\text{s.t.} \quad (8c).$$

Define $\boldsymbol{H}_{\mathrm{U}} \triangleq \boldsymbol{H}\boldsymbol{w}_{\mathrm{U}}\boldsymbol{w}_{\mathrm{U}}^{\dagger}\boldsymbol{H}^{\dagger}$, $\hat{\boldsymbol{G}}_{\mathrm{J}} \triangleq \hat{\boldsymbol{G}}\hat{\boldsymbol{G}}^{\dagger}$. The problem (14) is equivalent to

$$\max_{\boldsymbol{a}} \quad \min_{\hat{\boldsymbol{G}}_{\mathrm{J}}\in\Delta} \frac{p_{\mathrm{U}}\boldsymbol{a}^{\dagger}\boldsymbol{H}_{\mathrm{U}}\boldsymbol{a}}{\boldsymbol{a}^{\dagger}(p_{\mathrm{J}}\hat{\boldsymbol{G}}_{\mathrm{J}} + (p_{\mathrm{U}}\beta^2 c + \sigma^2)\boldsymbol{I})\boldsymbol{a}} \tag{15}$$

$$\text{s.t.} \quad (8c),$$

where $\Delta = \{\hat{\boldsymbol{G}}_{\mathrm{J}} = (\boldsymbol{G}+\boldsymbol{E})(\boldsymbol{G}+\boldsymbol{E})^{\dagger} | \|\boldsymbol{E}\| \leq \epsilon\}$. To find the weight vector $\boldsymbol{a}$ that maximizes the minimum achievable rate for all possible channel realizations, we first construct a convex hull as follows

$$\Gamma = \Big\{\sum_{t=1}^{T}\alpha_t\boldsymbol{G}_{\mathrm{J},t} | \sum_{t=1}^{T}\alpha_t = 1, \alpha_t \geq 0\Big\}, \tag{16}$$

Algorithm 1 The Proposed Algorithm for Solving (8)

Initialize: Convergence thresholds $\varepsilon > 0$, $\tau > 0$; Randomly generate feasible initial solutions $\boldsymbol{w}_{\mathrm{U}}^0$ and $\boldsymbol{a}^0$; Maximum allowable power $\{p_k\}_{k=1}^K$ for the K antenna clusters; The constructed convex hull Γ; Outer iteration index $\imath = 0$; Inner iteration index $\jmath = 0$; Calculate the achievable rate at the user R^0 by (5).
repeat
  $\imath = \imath + 1$;
  Obtain $\{\eta_k\}_{k=1}^K$ by solving (11);
  Calculate $\{\theta_k\}_{k=1}^K$ by $\theta_k = \eta_k P / \sum_{\kappa=1}^K \eta_\kappa p_\kappa$;
  Compute $\boldsymbol{\Upsilon}$ and $\boldsymbol{u}_{\max}$, and obtain $\boldsymbol{w}_{\mathrm{U}}^\imath$ by (13);
  repeat
    $\jmath = \jmath + 1$;
    Obtain $\{\alpha_t\}_{t=1}^T$ by (22);
    Calculate $\boldsymbol{a}^\jmath$ by (19);
  until $|\boldsymbol{a}^\jmath - \boldsymbol{a}^{\jmath-1}| < \tau$;
  Calculate the achievable rate $R^\imath$ based on $\boldsymbol{a}^\jmath$ and $\boldsymbol{w}_{\mathrm{U}}^\imath$;
until $\left|R^\imath - R^{\imath-1}\right| < \varepsilon$.

where $\boldsymbol{G}_{\mathrm{J},t}$ represents the t-th element sampled from the set of Δ, with T being the total number of samples. α_t denotes the t-th weighted coefficient. With the constructed convex hull, the original max-min problem can be converted into a min-max problem, which is illustrated in the following proposition.

Proposition 1: The max-min problem (15) is equivalent to the following min-max problem

$$\min_{\hat{\boldsymbol{G}}_{\mathrm{J}} \in \Gamma} \max_{\boldsymbol{a}} \frac{p_{\mathrm{U}} \boldsymbol{a}^\dagger \boldsymbol{H}_{\mathrm{U}} \boldsymbol{a}}{\boldsymbol{a}^\dagger (p_{\mathrm{J}} \hat{\boldsymbol{G}}_{\mathrm{J}} + (p_{\mathrm{U}} \beta^2 c + \sigma^2) \boldsymbol{I}) \boldsymbol{a}} \quad \text{s.t. (8c).} \tag{17}$$

Proof: See Appendix.

Based on *Proposition 1* and the expression of the convex hull in (16), the optimization problem can be reformulated as

$$\min_{\{\alpha_t\}_{t=1}^T} \max_{\boldsymbol{a}} \frac{p_{\mathrm{U}} \boldsymbol{a}^\dagger \boldsymbol{H}_{\mathrm{U}} \boldsymbol{a}}{\boldsymbol{a}^\dagger (p_{\mathrm{J}} \sum_{t=1}^T \alpha_t \boldsymbol{G}_{\mathrm{J},t} + (p_{\mathrm{U}} \beta^2 c + \sigma^2) \boldsymbol{I}) \boldsymbol{a}} \quad \text{s.t. (8c).} \tag{18}$$

Note that with given $\{\alpha_t\}_{t=1}^T$, the problem (18) follows from a generalized Rayleigh quotient form and the optimal solution is given by

$$\boldsymbol{a} = \mathrm{eig}(\boldsymbol{H}_{\mathrm{U}}, p_{\mathrm{J}} \sum_{t=1}^T \alpha_t \boldsymbol{G}_{\mathrm{J},t} + (p_{\mathrm{U}} \beta^2 c + \sigma^2) \boldsymbol{I}), \tag{19}$$

where the operator $\mathrm{eig}(\cdot,\cdot)$ represents the generalized eigenvector corresponding to the largest generalized eigenvalue of a matrix pair.

On the other hand, with given $\boldsymbol{a}$, we turn to determine the values of $\{\alpha_t\}_{t=1}^T$ to minimize the objective function in (18), such that the minimum achievable rate is obtained. From the Cauchy-Schwarz's inequality, it follows

$$\Big(\sum_{t=1}^T \alpha_t \boldsymbol{a}^\dagger \boldsymbol{G}_{\mathrm{J},t} \boldsymbol{a}\Big)^2 \le \Big(\sum_{t=1}^T \alpha_t^2\Big) \sum_{t=1}^T (\boldsymbol{a}^\dagger \boldsymbol{G}_{\mathrm{J},t} \boldsymbol{a})^2, \tag{20}$$

where the equality is satisfied in case

$$\frac{\alpha_1}{\boldsymbol{a}^\dagger \boldsymbol{G}_{\mathrm{J},1} \boldsymbol{a}} = \frac{\alpha_2}{\boldsymbol{a}^\dagger \boldsymbol{G}_{\mathrm{J},2} \boldsymbol{a}} = \cdots = \frac{\alpha_T}{\boldsymbol{a}^\dagger \boldsymbol{G}_{\mathrm{J},T} \boldsymbol{a}}. \tag{21}$$

Since we have $\sum_{t=1}^T \alpha_t = 1$, the values of $\{\alpha_t\}_{t=1}^T$ are given by

$$\alpha_t = \frac{\boldsymbol{a}^\dagger \boldsymbol{G}_{\mathrm{J},t} \boldsymbol{a}}{\sum_{t=1}^T \boldsymbol{a}^\dagger \boldsymbol{G}_{\mathrm{J},t} \boldsymbol{a}}. \tag{22}$$

The overall algorithm for optimizing the transmitter's beamforming and the receiving weighting factors with imperfect jamming channel is summarized in Algorithm 1.

C. Complexity and Convergence Analysis

The per-iteration complexity of Algorithm 1 is dominated by the transmit beamforming subproblem (steps 4-6) and receive weighting subproblem (steps 9-10). Solving (11) via SDP costs $\mathcal{O}(N^3)$, and eigenvalue decomposition (13) costs $\mathcal{O}(N^3)$. In addition, the generalized eigenvalue problem (19) costs $\mathcal{O}(L^3)$. Therefore, the total per-iteration complexity is $\mathcal{O}(N^3 + L^3)$. Moreover, as shown in Fig. 1, the proposed algorithm converges within 4 iterations, demonstrating the high efficiency. Compared with conventional scheme using CVX and SDPT3, of which the computational complexity is $\mathcal{O}(\sqrt{K}(N+L+\ell)^3 \log \frac{1}{\xi})$, where ξ is the target accuracy and $\ell \ge 2$ denotes the number of auxiliary variables, the proposed scheme achieves significant computational complexity reduction.

Regarding the convergence, the proposed Algorithm 1 belongs to AO framework. Its convergence is ensured by two properties, i.e., monotonic improvement and bounded objective. Specifically, each iteration solves subproblems (9) and (14) to global optimality, guaranteeing $R^{(i)}(\boldsymbol{w}_{\mathrm{U}}^{(i)}, \boldsymbol{a}^{(i)}) \le R^{(i+1)}(\boldsymbol{w}_{\mathrm{U}}^{(i+1)}, \boldsymbol{a}^{(i)}) \le R^{(i+1)}(\boldsymbol{w}_{\mathrm{U}}^{(i+1)}, \boldsymbol{a}^{(i+1)})$. Since the achievable rate is upper-bounded, from the monotone convergence theorem for bounded sequences, the algorithm converges to a stationary point.

IV. Numerical Results

In this section, we numerically evaluate the anti-jamming performance of the proposed scheme. The variance of the noise is $\sigma^2 = -110$ dBm. The numbers of the fixed antennas at the transmitter and the jammer are $N = 4$ and $M = 4$, respectively. In addition, the antennas at the transmitter are divided into two clusters, i.e., $K = 2$, and the power constraints are $p_1 = 0.2$, $p_2 = 0.8$. The convergence thresholds are $\varepsilon = \tau = 10^{-4}$. For comparison, the conventional fixed-position antenna (FPA)-based anti-jamming schemes relying on zero-forcing (ZF), minimum mean square error (MMSE), FAS-inspired combining (FIC) are considered as the benchmark schemes. In the ZF and MMSE schemes, the receive combining vectors are designed as $\boldsymbol{a}_{\mathrm{ZF}} = \frac{(\boldsymbol{I} - \hat{\boldsymbol{G}}(\hat{\boldsymbol{G}}^\dagger \hat{\boldsymbol{G}})^{-1} \hat{\boldsymbol{G}}^\dagger) \boldsymbol{H} \boldsymbol{w}_{\mathrm{U}}}{\|(\boldsymbol{I} - \hat{\boldsymbol{G}}(\hat{\boldsymbol{G}}^\dagger \hat{\boldsymbol{G}})^{-1} \hat{\boldsymbol{G}}^\dagger) \boldsymbol{H} \boldsymbol{w}_{\mathrm{U}}\|}$, $\boldsymbol{a}_{\mathrm{MMSE}} = \frac{(p_{\mathrm{J}} \hat{\boldsymbol{G}} \hat{\boldsymbol{G}}^\dagger + (p_{\mathrm{U}} \beta^2 c + \sigma^2) \boldsymbol{I})^{-1} \boldsymbol{H} \boldsymbol{w}_{\mathrm{U}}}{\|(p_{\mathrm{J}} \hat{\boldsymbol{G}} \hat{\boldsymbol{G}}^\dagger + (p_{\mathrm{U}} \beta^2 c + \sigma^2) \boldsymbol{I})^{-1} \boldsymbol{H} \boldsymbol{w}_{\mathrm{U}}\|}$, respectively. The optimization of the transmit beamforming follows a similar procedure as in Section III-A. In the FIC scheme, it applies the same robust combining strategy derived in Section III-B. However, it is implemented on a conventional FPA array with $\frac{\lambda}{2}$ spacing.

This article has been accepted for publication in IEEE Transactions on Vehicular Technology. This is the author's version which has not been fully edited and content may change prior to final publication. Citation information: DOI 10.1109/TVT.2025.3643346

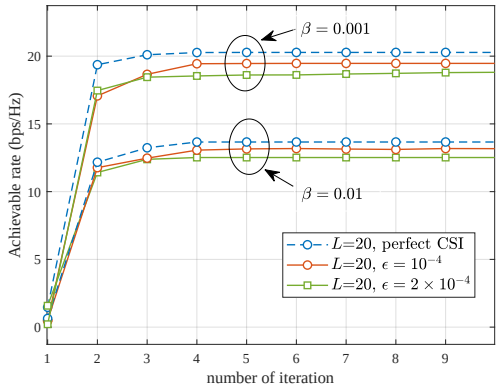

Fig. 1. Achievable rate versus the iteration, where $p_{\mathrm{U}} = 0$ dBm and $p_{\mathrm{J}} = 30$ dBm.

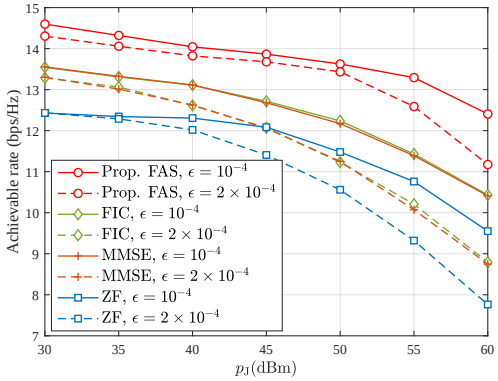

Fig. 2. Achievable rate versus the jamming power, where $L = 20$, $\beta = 0.001$, $p_{\mathrm{U}} = -20$ dBm.

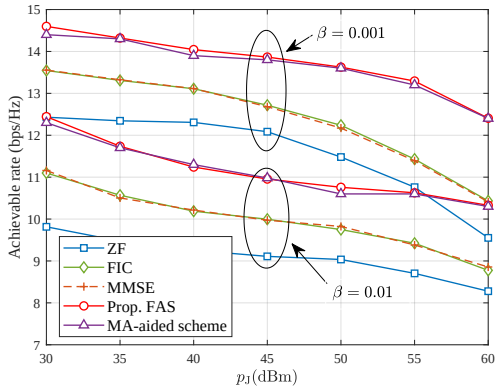

Fig. 3. Achievable rate versus the jamming power, where $L = 20$, $p_{\mathrm{U}} = -20$ dBm, $\epsilon = 10^{-4}$.

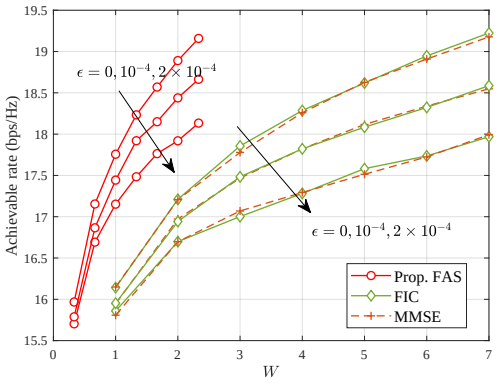

Fig. 4. Achievable rate versus the antenna length, where $p_{\mathrm{U}} = 0$ dBm, $p_{\mathrm{J}} = 30$ dBm, $\beta = 0.001$.

In addition, to provide a comparison with a contemporary reconfigurable antenna approach, we have included results from the recent MA-aided anti-jamming scheme proposed in [22], which also leveraged antenna mobility for resisting jamming signals.

First, we evaluate the convergence performance of the proposed algorithm. The transmit powers of the useful signal and the jamming are set as $p_{\mathrm{U}} = 0$ dBm, and $p_{\mathrm{J}} = 30$ dBm, respectively. Fig. 1 depicts the achievable rate versus the iteration number under varying levels of ISI and jamming channel uncertainty. For all cases, the proposed algorithm converges rapidly within 4 iterations, achieving stability regardless of imperfections like ISI coefficient and channel error bound. This highlights the computational efficiency of the semi-closed-form solutions derived in the proposed scheme.

Second, we illustrate the improvement in the achievable rate compared to the conventional FPA based anti-jamming schemes. Figs. 2 and 3 analyze the achievable rate versus jamming power, emphasizing FAS's dominance over benchmarks in mitigating interference. Both figures use $L = 20$ ports for FAS, while benchmark schemes employ 9 antennas to match the same antenna length, i.e., 4λ with $W = 4$. In addition, the MA-aided anti-jamming scheme employs 4 antenna elements. From Fig. 2, FAS consistently achieves higher rates than benchmark across all p_{J} levels. For instance, at $p_{\mathrm{J}} = 45$ dBm and $\epsilon = 10^{-4}$, FAS attains 13.8 bps/Hz, while the conventional FPA-based FIC and MMSE schemes only reach 12.7 bps/Hz. This 8% improvement stems from FAS's ability to exploit spatial diversity via rapid port switching, which suppresses jamming signals by combining differently faded receptions. The conventional schemes constrained by fixed antenna positions, cannot adapt dynamically and suffers from limited spatial degrees of freedom. From Fig. 3, FAS demonstrates superior robustness to ISI. With 1% and 0.1% ISI, FAS maintains a stable achievable rate gain over the conventional FPA benchmarks. Compared with the MA scheme, our single-RF-chain FAS receiver can achieve comparable performance to a 4-antenna, 4-RF-chain MA system, which demonstrates the hardware efficiency and compactness of our proposed design. This gain is primarily because the dense port layout of the FAS unlocks a much higher effective spatial diversity order than is possible with a small number of physically separated MA elements.

Fig. 4 evaluates achievable rate versus antenna length, revealing FAS's hardware advantages over FPA. FAS with port spacing $\frac{\lambda}{6}$ achieves higher rates with fewer resources. At $W = 1$ and $\epsilon = 2 \times 10^{-4}$, FAS delivers 17.15 bps/Hz, while FPA with identical antenna length only achieves 15.8 bps/Hz. This gap widens as W increases. Critically, FAS outperforms conventional schemes even at smaller antenna lengths, making it ideal for space-constrained devices like UAVs or IoT sensors. FAS requires only one RF chain,

reducing hardware costs and power consumption, while FPA needs multiple RF chains and antennas to match performance.

V. Conclusion

In this paper, we proposed an anti-jamming scheme based on the FAS. To improve the spatial degrees-of-freedom, the active port of the FAS rapidly switches in one symbol duration such that multiple received signals can be combined to mitigate the jamming while enhancing the desired signal. We maximized the achievable rate by transmit beamforming and receive combining, in which semi-closed-form solutions were derived. Numerical results underscore the proposed FAS as a transformative solution for anti-jamming communications, combining computational efficiency, robustness, and hardware economy to surpass conventional approaches.

Appendix

We first prove that the following two minimization problems are equivalent to each other

$$\min_{\hat{\boldsymbol{G}}_{\mathrm{J}}\in\Delta} \frac{p_{\mathrm{U}}\boldsymbol{a}^{\dagger}\boldsymbol{H}_{\mathrm{U}}\boldsymbol{a}}{\boldsymbol{a}^{\dagger}(p_{\mathrm{J}}\hat{\boldsymbol{G}}_{\mathrm{J}}+\gamma^2\boldsymbol{I})\boldsymbol{a}} = \min_{\hat{\boldsymbol{G}}_{\mathrm{J}}\in\Gamma} \frac{p_{\mathrm{U}}\boldsymbol{a}^{\dagger}\boldsymbol{H}_{\mathrm{U}}\boldsymbol{a}}{\boldsymbol{a}^{\dagger}(p_{\mathrm{J}}\hat{\boldsymbol{G}}_{\mathrm{J}}+\gamma^2\boldsymbol{I})\boldsymbol{a}}. \quad (23)$$

where $\gamma^2 \triangleq p_{\mathrm{U}}\beta^2 c+\sigma^2$. Since the set Γ is a convex hull of the set Δ, we have $\Delta \subseteq \Gamma$ and thus $\max_{\hat{\boldsymbol{G}}_{\mathrm{J}}\in\Delta} \boldsymbol{a}^{\dagger}\hat{\boldsymbol{G}}_{\mathrm{J}}\boldsymbol{a} \leq \max_{\hat{\boldsymbol{G}}_{\mathrm{J}}\in\Gamma} \boldsymbol{a}^{\dagger}\hat{\boldsymbol{G}}_{\mathrm{J}}\boldsymbol{a}$, which yields

$$\min_{\hat{\boldsymbol{G}}_{\mathrm{J}}\in\Delta} \frac{p_{\mathrm{U}}\boldsymbol{a}^{\dagger}\boldsymbol{H}_{\mathrm{U}}\boldsymbol{a}}{\boldsymbol{a}^{\dagger}(p_{\mathrm{J}}\hat{\boldsymbol{G}}_{\mathrm{J}}+\gamma^2\boldsymbol{I})\boldsymbol{a}} \geq \min_{\hat{\boldsymbol{G}}_{\mathrm{J}}\in\Gamma} \frac{p_{\mathrm{U}}\boldsymbol{a}^{\dagger}\boldsymbol{H}_{\mathrm{U}}\boldsymbol{a}}{\boldsymbol{a}^{\dagger}(p_{\mathrm{J}}\hat{\boldsymbol{G}}_{\mathrm{J}}+\gamma^2\boldsymbol{I})\boldsymbol{a}}. \quad (24)$$

On the other hand, for any matrix $\hat{\boldsymbol{G}}_{\mathrm{J}} \in \Gamma$, the equality $\boldsymbol{a}^{\dagger}\hat{\boldsymbol{G}}_{\mathrm{J}}\boldsymbol{a} = \sum_{t=1}^{T} \alpha_t \boldsymbol{a}^{\dagger}\hat{\boldsymbol{G}}_{\mathrm{J},t}\boldsymbol{a}$ holds, where $\sum_{t=1}^{T} \alpha_t = 1$ and $\alpha_t > 0$. Therefore, there exists a matrix $\hat{\boldsymbol{G}}_{\mathrm{J},t} \in \Delta$ satisfying $\boldsymbol{a}^{\dagger}\hat{\boldsymbol{G}}_{\mathrm{J},t}\boldsymbol{a} \geq \boldsymbol{a}^{\dagger}\hat{\boldsymbol{G}}_{\mathrm{J}}\boldsymbol{a}$, such that

$$\min_{\hat{\boldsymbol{G}}_{\mathrm{J}}\in\Delta} \frac{p_{\mathrm{U}}\boldsymbol{a}^{\dagger}\boldsymbol{H}_{\mathrm{U}}\boldsymbol{a}}{\boldsymbol{a}^{\dagger}(p_{\mathrm{J}}\hat{\boldsymbol{G}}_{\mathrm{J}}+\gamma^2\boldsymbol{I})\boldsymbol{a}} \leq \min_{\hat{\boldsymbol{G}}_{\mathrm{J}}\in\Gamma} \frac{p_{\mathrm{U}}\boldsymbol{a}^{\dagger}\boldsymbol{H}_{\mathrm{U}}\boldsymbol{a}}{\boldsymbol{a}^{\dagger}(p_{\mathrm{J}}\hat{\boldsymbol{G}}_{\mathrm{J}}+\gamma^2\boldsymbol{I})\boldsymbol{a}}. \quad (25)$$

From (24) and (25), we prove the equivalence in (23), and the objective function of (15) can be transformed into

$$\max_{\boldsymbol{a}} \min_{\hat{\boldsymbol{G}}_{\mathrm{J}}\in\Gamma} \frac{p_{\mathrm{U}}\boldsymbol{a}^{\dagger}\boldsymbol{H}_{\mathrm{U}}\boldsymbol{a}}{\boldsymbol{a}^{\dagger}(p_{\mathrm{J}}\hat{\boldsymbol{G}}_{\mathrm{J}}+\gamma^2\boldsymbol{I})\boldsymbol{a}}. \quad (26)$$

Next, we prove that the max-min problem (26) can be converted to a min-max problem using the saddle point property [23]. Since the set Γ is convex, the objective function in (26) is convex with respect to $\hat{\boldsymbol{G}}_{\mathrm{J}} \in \Gamma$ for any given $\boldsymbol{a}$. According to [23], we have a saddle point $(\boldsymbol{a}^{\circ}, \hat{\boldsymbol{G}}_{\mathrm{J}}^{\circ})$ that follows

$$\frac{p_{\mathrm{U}}\boldsymbol{a}^{\dagger}\boldsymbol{H}_{\mathrm{U}}\boldsymbol{a}}{\boldsymbol{a}^{\dagger}(p_{\mathrm{J}}\hat{\boldsymbol{G}}_{\mathrm{J}}^{\circ}+\gamma^2\boldsymbol{I})\boldsymbol{a}} \leq \frac{p_{\mathrm{U}}(\boldsymbol{a}^{\circ})^{\dagger}\boldsymbol{H}_{\mathrm{U}}\boldsymbol{a}^{\circ}}{(\boldsymbol{a}^{\circ})^{\dagger}(p_{\mathrm{J}}\hat{\boldsymbol{G}}_{\mathrm{J}}+\gamma^2\boldsymbol{I})\boldsymbol{a}^{\circ}}. \quad (27)$$

From the saddle point property in the minimax theory, we know that the maximize and minimize operators in (26) can be exchanged in order, since both the two problems have the same solution at the saddle point $(\boldsymbol{a}^{\circ}, \hat{\boldsymbol{G}}_{\mathrm{J}}^{\circ})$, which completes the proof.

References

[1] H. Pirayesh and H. Zeng, "Jamming attacks and anti-jamming strategies in wireless networks: a comprehensive survey," *IEEE Commun. Surveys Tuts.*, vol. 24, no. 2, pp. 767-809, 2nd Quart., 2022.

[2] B. He, Z. Chen, J. Luo et al., "Towards secure semantic transmission in the era of GenAI: A diffusion-based framework," 2025, *arXiv: 2505.05724*. [Online]. Available: https://arxiv.org/abs/2505.05724.

[3] T. T. Do, E. Björnson, E. G. Larsson, and S. M. Razavizadeh, "Jamming resistant receivers for the massive MIMO uplink," *IEEE Trans. Inf. Forensics Security*, vol. 13, no. 1, pp. 210–223, Jan. 2018.

[4] W. K. New, K.-K. Wong, H. Xu, et al., "A tutorial on fluid antenna system for 6G networks: encompassing communication theory, optimization methods and hardware designs," *IEEE Commun. Surveys & Tuts.*, early access, 2024.

[5] A. Besoli and F. De Flaviis, "A multifunctional reconfigurable pixeled antenna using MEMS technology on printed circuit board," *IEEE Trans. Antennas Propag.*, vol. 59, no. 12, pp. 4413–4424, Dec. 2011.

[6] S. Basbug, "Design and synthesis of antenna array with movable elements along semicircular paths," *IEEE Antennas Wireless Propag. Lett.*, vol. 16, pp. 3059–3062, 2017.

[7] K.-K. Wong, A. Shojaeifard, K.-F. Tong, et al., "Fluid antenna systems," *IEEE Trans. Wireless Commun.*, vol. 20, no. 3, pp. 1950–1962, Mar. 2021.

[8] W. K. New, et al., "Fluid antenna system: New insights on outage probability and diversity gain," *IEEE Trans Wireless Commun.*, vol. 23, no. 1, pp. 128-140, 2024.

[9] H. Xu, K.-K. Wong, W. K. New, et al., "Capacity maximization for FAS-assisted multiple access channels," *IEEE Trans. Commun.*, early access, 2025.

[10] H. Xu, K.-K. Wong, W. K. New, et al., "Coding-enhanced cooperative jamming for secret communication in fluid antenna systems," *IEEE Commun. Lett.*, vol. 28, no. 9, 2024.

[11] B. Tang, H. Xu, K.-K. Wong, et al., "Fluid antenna enabling secret communications," *IEEE Commun. Lett.*, vol. 27, no. 6, pp. 1491-1495, 2023.

[12] C. Wang et al., "Fluid antenna system liberating multiuser MIMO for ISAC via deep reinforcement learning," *IEEE Trans. Wireless Commun.*, vol. 23, no. 9, pp. 10879-10894, Sept. 2024.

[13] C. Wang, Z. Li, K. -K. Wong, et al., "AI-empowered fluid antenna systems: Opportunities, challenges, and future directions," *IEEE Wireless Commun.*, vol. 31, no. 5, pp. 34-41, Oct. 2024.

[14] W. K. New et al., "An information-theoretic characterization of MIMO-FAS: Optimization, diversity-multiplexing tradeoff and q-outage capacity," *IEEE Trans. Wireless Commun.*, vol. 23, no. 6, 2024.

[15] H. Ma, W. Mei, X. Wei, et al., "Robust movable-antenna position optimization with imperfect CSI for MISO systems, *IEEE Commun. Lett.*, early access, 2025.

[16] W. Mei, X. Wei, B. Ning, et al., "Movable-antenna position optimization: a graph-based approach," *IEEE Wireless Commun. Lett.*, vol. 13, no. 7, pp. 1853-1857, 2024.

[17] Y. Wu, D. Xu, D. W. K. Ng, et al., "Movable antenna-enhanced multiuser communication: jointly optimal discrete antenna positioning and beamforming," *IEEE Global Communications Conference*, Kuala Lumpur, Malaysia, 2023.

[18] X. Shao, R. Zhang, Q. Jiang et al., "6D movable antenna enhanced wireless network via discrete position and rotation optimization," *IEEE J. Sel. Areas Commun.*, vol. 43, no. 3, pp. 674-687, 2025.

[19] S. Gong, C. Xing, X. Zhao, et al., "Unified IRS-aided MIMO transceiver designs via majorization theory," *IEEE Trans. Signal Process.*, vol. 69, pp. 3016-3032, 2021.

[20] K. Malek, K. Abla and A. Mohamed-Slim, "A new analytical approximation of the fluid antenna system channel," *IEEE Trans. Wireless Commun.*, vol. 22, no. 12, pp. 8843-8858, 2023.

[21] W. -T. Li, et al., "60-GHz 5-bit phase shifter with integrated VGA phase-error compensation," *IEEE Trans. Microwave Theory Tech.*, vol. 61, no. 3, pp. 1224-1235, 2013.

[22] Y. Guo, J. Luo, Y. Sun, et al., "Movable antenna array design for jamming mitigation," in *IEEE Int. Conf. Commun. Workshops (ICC Workshops)*, Montreal, QC, Canada, 2025, pp. 19-25.

[23] S. Verdu and H. Poor, "On minimax robustness: A general approach and applications," *IEEE Trans. Inf. Theory*, vol. IT-30, no. 2, pp. 328-340, 1984.